JOURNAL OF Materials CHEMISTRY

Calculating the helical twisting power of chiral dopants†

Mark R. Wilson* and David J. Earl

Department of Chemistry, University of Durham, South Road, Durham, UK DH1 3LE. E-mail: mark.wilson@durham.ac.uk; Fax: +44 191 386 1127; Tel: +44 191 374 4634

Received 19th April 2001, Accepted 11th July 2001
First published as an Advance Article on the web 2nd October 2001

This paper describes a Monte Carlo simulation technique designed to predict the sign and magnitude of the helical twisting power, β_M, of a chiral material. The method calculates the chemical potential difference, $\Delta\mu$, between a chiral dopant and its enantiomer when they are placed in a twisted nematic solvent. In the low concentration limit, $\Delta\mu$ is directly proportional to β_M. In the simulations presented, the chiral dopants are represented by atomistic models and a generic twisted nematic solvent composed of soft repulsive spherocylinders is employed. A free energy perturbation method is used to calculate $\Delta\mu$. Calculations are presented for five different dopant molecules with a wide range of helical twisting powers.

Introduction

If a *nematic* liquid crystal is doped with a low concentration of chiral material, then a *chiral nematic* phase is formed with a helical pitch, P, which is inversely proportional to the concentration of the chiral dopant. Experimental work points to the fact that different dopant molecules have widely different abilities to twist a nematic phase, and this is normally characterized by defining a *macroscopic helical twisting power* (HTP) β_M:[1]

$$\beta_M = (Pc_w r)^{-1} \quad (1)$$

where c_w is the weight concentration of chiral dopant and r defines its enantiomeric purity. Depending on the material concerned, the sign of β_M can be either positive (right-handed helix) or negative (left-handed helix). Two pure enantiomers of the same material will always have the same magnitude of β_M but opposite signs.

There are important technological uses for chiral dopant materials. They are used in low concentrations in twisted nematic displays, and in chiral films for use with displays. They can also be used in polarization sensitive polymer films[2] and thermally addressed display materials.[3] In many applications however, limits on solubility of the dopant, or specific material requirements mean that only small concentrations of chiral dopants can be employed. Consequently, there has been considerable interest in the synthesis of materials with high β_M values. However, this can be an extremely difficult task to achieve. There are no easy rules to follow to predict how the molecular structure of a chiral dopant is related to the helical twisting power it induces. Small changes in structure can lead to large changes in β_M.[4,5] These large changes apparently arise because chiral solute molecules with slightly different shapes can induce significant differences in the local orientational order of the solvent molecules around them. This in turn induces different amounts of twist in the bulk solvent. It is clear therefore that a theoretical method that can predict helical twisting values reliably would be extremely valuable. It would improve our understanding of why some molecules have large HTPs and some do not, and it could be used as a way of sifting through many trial molecular structures prior to attempting a difficult synthetic pathway. The latter encompasses one of the key aims of modern theoretical chemistry: to do *molecular engineering*, *i.e.* to predict key material properties based only on a prior knowledge of chemical structure and molecular interactions.

A number of workers have attempted to provide a theoretical framework for predicting HTPs. Prominent is the work of Nordio, Ferrarini and co-workers who provide an interesting theoretical model for predicting HTPs based on a mean field description of the interactions between a chiral solute molecule and a liquid crystal solvent.[6–9] Their model has shown considerable success, though does not appear to work in all cases. Cook and Wilson[10] recently formulated a different technique for obtaining HTPs of chiral dopants based on some earlier work by Allen.[11] This method involves simulations of a chiral dopant molecule in a twisted nematic solvent using an efficient Monte Carlo (MC) simulation program. The MC simulations are used to compute the difference in chemical potential, $\Delta\mu$, between a chiral solute and its enantiomer immersed in the same *twisted nematic* solvent. $\Delta\mu$ is directly proportional to β_M, and, given a value for the twist elastic constant, K_2, an absolute value for β_M can be predicted. The Cook–Wilson method is revisited in this article. We consider simulations in a generic solvent composed of soft repulsive spherocylinder molecules. We do this because this particular solvent is relatively cheap to simulate, and in many cases HTP values do not depend critically on the nature of the solvent. (We discuss the experimental cases where HTPs have been influenced by the solvent later in the article.) However, our method is not limited to simple phenomenological models for the solvent, and can be extended relatively easily to solvents that are represented by fully atomistic potentials.

The format of this paper is as follows. In section 2, we outline the theory behind this method of calculating HTPs. In section 3, we describe the soft repulsive spherocylinder solvent and some molecular dynamics simulations along an isochore, which allow us to obtain a suitable state-point for use in the HTP simulations. In section 4, we describe Monte Carlo free energy perturbation simulations used to obtain HTPs in the presence of the soft spherocylinder solvent, and in section 5 we describe the results arising from these calculations. Finally, in section 6 we make some general comments about the strengths and weaknesses of our method and indicate the ways in which it can be extended with further work.

†Basis of a presentation given at Materials Discussion No. 4, 11–14 September 2001, Grasmere, UK.

 DOI: 10.1039/b103520g

Theory

When the concentration of chiral dopant is small, then, following the de Gennes definition,[1] the equilibrium wavevector k_0 of the twisted phase is linearly dependent on the concentration of solute molecules [eqn. (2)].

$$k_0 = \frac{2\pi}{P_0} = 4\pi\beta\rho \tag{2}$$

Here, $\rho = N/V$ is the number density of dopant molecules and the constant of proportionality β is defined as the *microscopic* helical twisting power.[1] (We note in passing that de Gennes definition of β is not the same as that of the usual quantity β_M of eqn. (1) that is measured experimentally, but β can easily be converted into β_M.) If a uniformly twisted nematic with wavevector $k = 2\pi/P$ is doped with small numbers (N_+ and N_-) of a chiral dopant (with a microscopic HTP of $\pm\beta$), then there will be an elastic contribution to the free energy that arises from distortions from the uniformly twisted state[11] [eqn. (3)]:

$$\Delta F = \frac{1}{2} V K_2 \left(k - \frac{4\pi\beta}{V} [N_+ - N_-] \right)^2 \tag{3}$$

where V is the volume of the system and K_2 is the twist elastic constant. Following Allen,[11] in the limit of infinite dilution (N_-, $N_+ \rightarrow 0$),

$$\mu_- - \mu_+ = \frac{\partial F}{\partial N_-} - \frac{\partial F}{\partial N_+} = 8\pi\beta K_2 k \tag{4}$$

so that

$$\beta = \frac{\Delta\mu}{8\pi K_2 k} \tag{5}$$

Hence (for low values of k), in the low concentration limit, we would be expected to be able to obtain values for β from a measurement of the chemical potential difference between two enantiomers in a uniformly twisted nematic solvent with a twist elastic constant of K_2.

Simulations of soft repulsive spherocylinders

The soft repulsive spherocylinder (SRS) potential is computationally efficient, usually requiring 3–4 times less computer power than the more familiar single-site Gay–Berne model. It is therefore a useful solvent to employ in the calculations of helical twisting power described in section 4. However, with the exception of some rather preliminary work by Japanese workers,[12–14] little is known about the phase diagram of this system. Consequently, we carried out molecular dynamics studies for a whole series of isochores of a SRS system with $L/D = 4$ (Fig. 2). The results of these studies will be described in full in a later work;[15] here we present the results for one isochore, from which we obtained a suitable nematic state-point for use in section 4.

675 SRS molecules were studied. The molecules had a purely repulsive short range pair potential of the form

$$U_{ij} = \begin{cases} 4\varepsilon \left[\left(\frac{\sigma_0}{d_{ij}} \right)^{12} - \left(\frac{\sigma_0}{d_{ij}} \right)^{6} + \frac{1}{4} \right], & d_{ij} < d_{\text{cut}} \\ 0, & d_{ij} \geq d_{\text{cut}} \end{cases} \tag{6}$$

where $\sigma_0 = D$ is the diameter of the spherocylinder, d_{ij} is the shortest separation between hard lines of length L that run through the middle of each spherocylinder (see Fig. 1) and $d_{\text{cut}} = 2^{1/6}\sigma_0$. The distance dependence of the pair potential is shown in Fig. 2. The SRS molecules were initially placed, completely aligned, in a simulation box of cubic dimensions subject to periodic boundary conditions. A molecular dynamics (MD) simulation using a Berendsen thermostat NVT ensemble

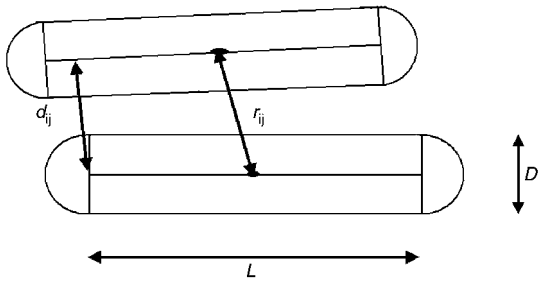

Fig. 1 Schematic diagram defining the soft repulsive spherocylinder model.

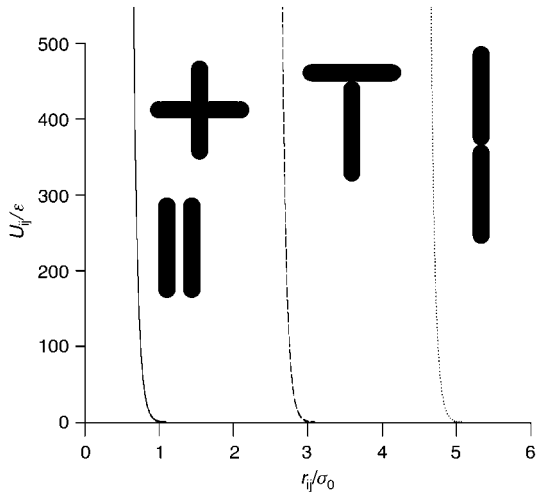

Fig. 2 The SRS pair potential for four fixed orientations of spherocylinders.

was used to 'melt' the system until the isotropic phase was obtained. The NVT ensemble was then used to sequentially reduce the temperature of the system to desired levels. Equilibration was generally achieved at each temperature after 1–5 $\times$ 10^5 steps. Further, MD simulations in the NVE ensemble were then used to equilibrate the sample at each state point and the average temperature, pressure and order parameter, S_2, were computed over production runs of 0.5–2 $\times$ 10^5 steps.

The results for the uniaxial nematic order parameter

$$S_2 = \left\langle \frac{3}{2}\cos^2\theta - \frac{1}{2} \right\rangle \tag{7}$$

as a function of temperature are shown in Fig. 3. In eqn. (7), the angular brackets indicate an ensemble average and θ is the angle between a molecule and the nematic director. For

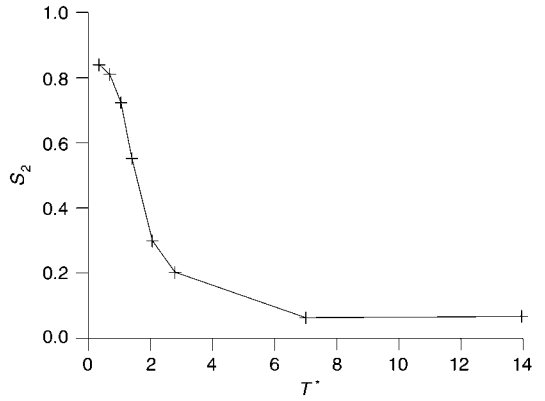

Fig. 3 The uniaxial nematic order parameter, S_2 as a function of reduced temperature, T^*, for a reduced density of $\rho^* = 0.131857$.

constant volume simulations the system goes through a two phase region, but is in a well-defined nematic phase between $T^* = 1.5$ and $T^* = 1.0$. A state point of $T^* = 1.3$ (corresponding to $S_2 = 0.67$) was chosen for the HTP calculations in section 4. We note in passing that the order parameter does not drop sharply to zero in Fig. 3. This is caused by the two-phase region seen in these NVT simulations. At high temperatures the small residual orientational order is typical of that seen in simulations conducted with relatively small numbers of particles.

In order to carry out the helical twisting power calculations it is necessary to have a twisted nematic solvent. In order to do this the twisted periodic boundary conditions of Allen and Masters[16] can be employed. Here, molecules in the neighbouring simulation box ($+z$ direction) are rotated through 90 degrees about the z axis with respect to their coordinates and orientations in the original box (and those in the neighbouring box in the opposite ($-z$) direction are rotated through -90 degrees). For $T^* = 1.3$, we tested whether the twist imposed by the periodic box had any significant effect on the ordering of the model fluid. Using Monte Carlo simulations of the SRS fluid (described in section 4) we obtained essentially identical results for the nematic order parameter in an untwisted system and the chiral nematic order parameter in a 90 degrees twisted system. The values of these order parameters were in agreement with the molecular dynamics results.

Calculations of HTPs

Allen[11] has used eqn. (5) to obtain values of β for dimers consisting of two touching prolate ellipsoids of axial ratio $e = 5$ within a fluid of similar monomeric ellipsoids. In that work an explicit expression was obtained for the excess chemical potential of a dimer composed of two hard ellipsoids in contact in a twisted nematic phase of hard ellipsoids.[17] However, eqn. (5) is not restricted to systems where explicit expressions can be derived for the chemical potential. For example, $\Delta\mu$ is equivalent to the free energy change in converting one mole of chiral solute into its mirror image in the presence of a twisted nematic solvent at infinite dilution. This quantity can be obtained in a number of ways. One simple pathway involves using statistical perturbation theory[18,19] to grow an enantiomer into an excess of twisted nematic solvent and measuring the free energy change for that process, followed by a comparison between this quantity and that obtained for the same calculation on the enantiomer. In the simplest possible case, we write the internal energy of the combined solvent/solute system as eqn. (8)

$$\begin{aligned} E_\lambda = U_{\mathrm{tot}} = U^{\mathrm{solute}} \\ + \sum_{i=1}^{N_{\mathrm{solvent}}} \sum_{j<i}^{N_{\mathrm{solvent}}} U_{ij}^{\mathrm{solvent}} \\ + \sum_{i=1}^{N_{\mathrm{solute}}} \sum_{j=i}^{N_{\mathrm{solvent}}} U_{ij}^{\mathrm{solvent/solute}} \end{aligned} \tag{8}$$

where U^{solute} is the solute energy (a constant for a rigid solute molecule), $U_{ij}^{\mathrm{solvent}}$ (see ref. 20) is the solvent interaction energy [in this case given by the SRS interaction energy in eqn. (6)] and $U_{ij}^{\mathrm{solvent/solute}}$ is the solute–solvent interaction energy (defined below). In eqn. (8), the solute has N_{solute} atoms interacting with N_{solvent} solvent molecules, and a control parameter λ, which varies between 0 and 1, controls the growth of solute into the solvent (see below). In the spirit of the SRS potential, we have used a similar form for the interaction between a solute atom and a solvent molecule, such that eqn. (6) is followed with the distance d_{ij} becoming the shortest separation between a hard line through the middle of the spherocylinder and the centre of the atomic site. The usual combining rules are applied [eqn. (9) and (10)]

$$\sigma_0^{\mathrm{solute/solvent}} = \frac{\sigma_0^{\mathrm{atom}} + \sigma_0^{\mathrm{solvent}}}{2} \tag{9}$$

$$\varepsilon_0^{\mathrm{solute/solvent}} = \sqrt{\varepsilon_0^{\mathrm{atom}} \varepsilon_0^{\mathrm{solvent}}} \tag{10}$$

where ${\varepsilon_0}^{\mathrm{atom}}$ and ${\sigma_0}^{\mathrm{atom}}$ values for each atom type in the solute are taken from the values for these used in the OPLS-AA force field of Jorgensen.[21] The latter has been fitted to give excellent densities and heats of vaporization for small organic molecules. For ${\varepsilon_0}^{\mathrm{solvent}}$ we have used a value of 2.5583 kJ mol^{-1}, which for the reduced density of $\rho^* = 0.131857$ used in section 3, scales the reduced temperature of $T^* = 1.3$ to 400 K. A value of ${\sigma_0}^{\mathrm{solvent}} = 5.7$ Å was used to provide a generic solvent with an overall length ($5{\sigma_0}^{\mathrm{solvent}} = 28.5$ Å) that is in the typical range for many nematogens.

The free energy difference between two systems is given by eqn. (11)

$$\Delta F_{BA} = -k_B T \ln\langle \exp(-\Delta E_{BA}/k_B T)\rangle_A \tag{11}$$

where ΔE_{BA} is the energy difference between systems A and B and the angular brackets indicate an ensemble average over a simulation of system A. Eqn. (11) is only valid for two systems with similar Hamiltonians. Consequently the growth of an enantiomer into the twisted nematic solvent must be carried out in a series of separate simulations, using the dimensionless control parameter $0 \leqslant \lambda \leqslant 1$ to gradually perturb the system. In this work the values of ${\sigma_0}^{\mathrm{atom}}$ and ${\varepsilon_0}^{\mathrm{solute/solvent}}$ were both scaled by λ. Consequently, the growth of solute starts from an initial non-interacting point particle at $\lambda = 0$ and continues to produce a completed solute molecule at $\lambda = 1$. The total free energy change is summed from the individual components measured during each simulation

$$\begin{aligned} \Delta F^{\mathrm{solute/solvent}} = \\ \sum_{i=1}^{n} -k_B T \ln\langle \exp[-(E_{\lambda_{i+1}} - E_{\lambda_i})/k_B T]\rangle_{\lambda_i} \end{aligned} \tag{12}$$

Calculations were carried out on the molecules shown in Fig. 4. These same molecules have been used in the earlier study by Cook and Wilson using a Gay–Berne solvent.[10] For each molecule, the equilibrium lowest energy structure was computed by carrying out energy minimisation calculations using the MM2 force-field. This geometry was then turned into a Z-matrix prior to the MC calculations, and the exact geometry of the enantiomer was obtained by reversing the signs of the dihedral angles in the Z-matrix. These rigid geometries were then used in the subsequent MC studies. MC simulations were carried out using 513 SRS solvent molecules in a cuboidal cell of dimensions 1 : 1 : 2 for the state-point described in section 3, employing twisted periodic boundary conditions. A random rotation/translation of the solute molecule and each of the solvent molecules was attempted during each Monte Carlo cycle. Molecular orientations were represented in terms of quaternions and a random rotation was carried out using the approach described in refs. 22 and 23, with move sizes adjusted to give MC acceptance ratios in the range 35–55%. All simulations were conducted in the NVT ensemble at 400 K. Prior to the free energy calculations the solvent was well-equilibrated using 2×10^5 Monte Carlo cycles. 20 λ steps were carried out for each enantiomer (40 λ steps in total for each material) where $\lambda_i = (i/20)$, $i = 1, 20$. 4000 MC equilibration cycles and 20000 MC production cycles were employed at each value of λ.

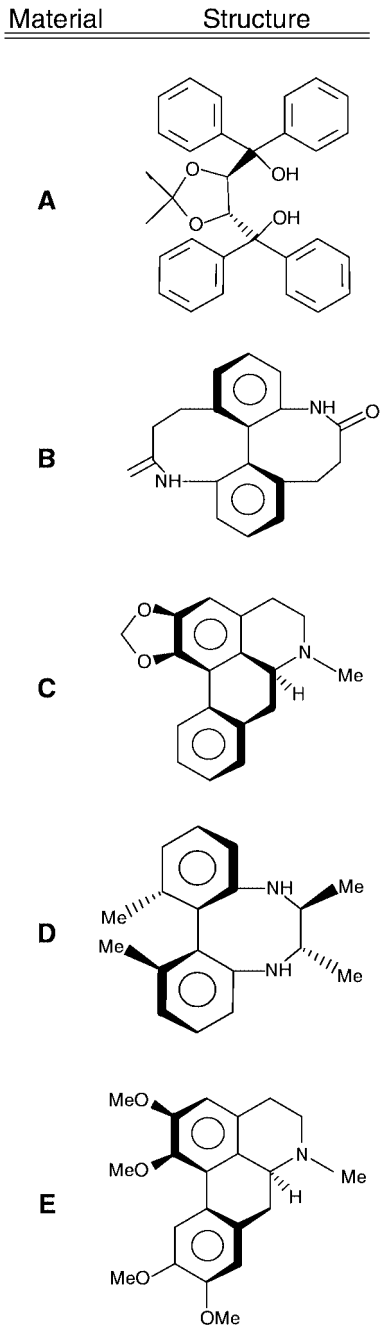

Fig. 4 The structures of the five chiral dopant molecules A–E investigated in this study.

HTP Results

The results from the free energy perturbation calculations are given in Table 1. In each case the free energy change is positive on account of the lack of attractive interactions in the model and the disruption in solvent structure caused by the growth of the solute molecule. This contrasts with free energy perturbation calculations for growth in a Gay–Berne (GB) solvent[10] where the overall free energy change is negative. For GB particles the disruption in solvent structure is more than compensated for by the solute–solvent interaction, which is strongly attractive. In the case of each molecule we are able to detect a preference for one or other of the enantiomers in terms of the magnitude of ΔF. In each case the smallest free energy change corresponds to the enantiomer that is predicted to induce a helical twist in a nematic solvent with the same twist sense as the periodic box. Unfortunately the errors for ΔF are rather large and this means that the errors associated with the calculated values of $\Delta\mu$ are large also. The latter are given in Table 2 along with HTP values from experiment. Because the SRS solvent is newly studied, there are (unlike the Gay–Berne solvent) no calculations of the twist elastic constant available. We have converted $\Delta\mu$ values to absolute values of β_M by choosing parameters for the molecular mass = 249.36 g mol^{-1} of the solvent (mass of 5CB) and $K_2 = 1.63 \times 10^{-11}$ J m^{-1}, such that they give the best fit to the experimental data. Calculated values of β_M have been included in Table 2 along with those obtained for a Gay–Berne solvent using a calculated value for the Gay–Berne twist elastic constant.[24]

Table 1 The overall free energy changes computed for the growth of each molecule shown in Fig. 4 and its mirror image

Molecule	ΔF/kJ mol^{-1} for configuration in Fig. 4	ΔF/kJ mol^{-1} for enantiomer
A	20.3 ± 0.4	20.9 ± 0.5
B	13.0 ± 0.3	13.9 ± 0.5
C	13.8 ± 0.3	15.1 ± 0.4
D	14.1 ± 0.1	13.8 ± 0.1
E	18.3 ± 0.4	18.3 ± 0.4

Discussion

The results presented in this paper and elsewhere[10] suggest that using the chemical potential difference between enantiomers in a twisted nematic solvent is a valuable theoretical approach for the calculation of helical twisting powers. For the materials studied, we have been able to predict the correct sign of the helical twisting power: an important prediction in its own right.

For the SRS solvent the predictions for the magnitude of β_M are less impressive than those for the Gay–Berne system. This is most likely to be because the errors for the free energy calculations are much larger for the SRS solvent: the double-wide sampling technique used for a Gay–Berne solvent in ref. 10 is not suitable for a harder SRS potential, and the errors in ΔF values must be addressed (see below) if this fluid is to be used to provide quantitative predictions for HTPs. If the free energy calculations can be improved the SRS mesogen should provide potentially a better solvent for these calculations than the Gay–Berne fluid used in ref. 10. Firstly, the SRS potential is 3–4 times computationally cheaper than the Gay–Berne potential. Secondly, the free energy changes for the SRS fluid should not be complicated by the long-range attractions of the Gay–Berne potential. Thirdly, it is likely that values of $\Delta\mu$ should be larger for the SRS fluid than for GB particles in ref. 10, because the longer spherocylinder particles should have a greater nematic twist elastic constant for the state-points studied. However, the latter could be

Table 2 Calculated values of $\Delta\mu$ and helical twisting powers for the molecules shown in Fig. 4. (The sign of β_M is specified for the enantiomer with the stereochemistry shown in Fig. 4.) The computed SRS results in column 4 are given along with values computed for a Gay–Berne solvent in column 5 in ref. 10

Molecule	$\Delta\mu$/ kJ mol^{-1}	β_M (Exp.)/ μm^{-1}	β_M (Comp. SRS)/ μm^{-1}	β_M (Comp. GB)/ μm^{-1}
A	0.61 ± 0.64	+104	+17 ± 18	+99.3
B	0.97 ± 0.56	+58	+43 ± 25	+69.0
C	1.30 ± 0.50	+24	+61 ± 23	+27.9
D	0.27 ± 0.14	−21	−13 ± 7	−26.7
E	0.02 ± 0.55	+8	+1 ± 20	0

remedied by use of longer Gay–Berne systems or parametrizations of the Gay–Berne potential with larger twist elastic constants. K_2 has yet to be measured independently for the spherocylinder fluid, but could be obtained from monitoring of wavevector-dependent fluctuations in the ordering tensor.[24]

In the current study, computational cost has limited the system size to 513 particles. However, eqn. (5) is valid in the low concentration limit and it would be highly desirable in future work to test the system size dependence of the results. If more accurate values for $\Delta\mu$ can be obtained in future calculations, it will be interesting to see if the different HTP values for each molecule are dependent on the nature of the solvent (GB or SRS). A number of workers have noted that HTP values do not vary significantly for chemically similar solvents. For this reason we believe that the crucial factor in determining HTPs is the molecular shape, rather than solvent–solute attractive interactions. The shape of the solute influences how solvent molecules pack around it, and in an untwisted nematic this will lead to a uniform twist in the bulk solvent. It will be interesting to test this prediction by looking at other single-site solvent models, and some work on this is already under way in our laboratory.

When the nature of the nematic solvents used for HTP measurements is chemically different, particularly with reference to differences in their electrostatic interactions, researchers have been able to detect solvent-induced differences in HTP values. It is even, in extreme cases, possible to obtain different signs for β_M.[5,25] In these cases solvent–solute interactions clearly do have an influence on helical twisting power. A likely scenario here is that particular conformations are chosen preferentially in different solvents and that different conformations can have different β_M values. There is some evidence for this effect in the work of Ferrarini *et al.*[26] However, it would be relatively easy to test this suggestion by studying different rigid conformations in a SRS solvent; or alternatively, by using flexible molecules, as an extension to the method presented here. We note that in using flexible molecules it would be important to ensure that accurate conformational averaging occurred for both enantiomers. This is likely to require substantially longer Monte Carlo runs for each free energy point. It would also be interesting to use the Monte Carlo method to study the relative populations of different enantiomers in different solvents. For example, to study the influence of dipolar solvents a point dipole could be incorporated into the SRS solvent. The solvent dipole would interact with bond dipoles within the flexible chiral solute.

It is possible also to represent the twisted nematic solvent completely atomistically. In this way, it would be possible to represent solvent–solute interactions faithfully. There is already a large body of evidence pointing to the ability of good quality atomistic calculations to represent mesogenic interactions accurately.[27–29] However, the drawback of atomistic calculations is their computational expense. Currently, such studies would require in the region of CPU months on today's standard workstations. Clearly the capability of sifting through a range of structures to look for the highest HTP value would not be available if a fully atomistic treatment of the solvent was used.

The free energy calculations used in this paper, were relatively simple to implement. However, they are clearly not the most sophisticated (or necessarily the best) approach to obtaining $\Delta\mu$ for a relatively hard potential model such as the SRS mesogen. More sophisticated free energy calculations are possible and many of these are applicable to the systems we have studied (for an excellent review of applicable methods see ref. 30). In addition, other more complicated free energy pathways are possible. An interesting approach involves taking a chiral dopant and gradually shrinking it, while simultaneously growing its enantiomer out from the centre of the original dopant. Alternative growth techniques, and the twin enantiomer approach are currently being investigated in our laboratory. Once these techniques have been implemented it will be interesting to compare the accuracy and computational expense of the method described here and the alternative molecular field theory approach of Ferrarini *et al.*[7–9] The latter is based on the structure of a single dopant molecule, the orienting strength of the nematic medium and the chirality order parameter; and therefore does not rely on implicit solvent molecules. This is both a weakness (in terms of not being able to take local solvent–solute interactions in to account), and a strength (in terms of computational cheapness). Further work is required in comparing the two methods.

Finally, the long term potential of the work presented here is the ability to extend to more realistic solvent models (as discussed above). In such studies changes in the statistical weight of each conformer that usually occur when entering an orientationally ordered phase will be taken into account automatically, as will any differences in HTPs arising from specific solvent–solute interactions. Such studies should yield accurate HTPs in all cases.

Acknowledgements

The authors wish to thank EPSRC for providing computer time on a Cray T3E (grant GR/M16023) and through the purchase of workstations (grant GR/M21676). DJE wishes to thank the EPSRC and Merck NS-BC for providing a research studentship (2000–2003), and Merck NS-BC for the gift of a DEC 433 a.u. workstation.

References

1 P. G. de Gennes and J. Prost, in *The Physics of Liquid Crystals*, 2nd edition, Oxford University Press, Oxford, 1993, Ch. 6.
2 P. van de Witte, E. E. Neuteboom, M. Brehmer and J. Lub, *J. Appl. Phys.*, 1999, **85**, 7517.
3 H. Yang, H. Yamane, H. Kikuchi, H. Yamane, G. Zhang, X. F. Chen and K. Tisato, *J. Appl. Polym. Sci.*, 1999, **73**, 623.
4 C. Stützer, W. Weissflog and H. Stegmeyer, *Liq. Cryst.*, 1996, **21**, 557.
5 S. N. Yarmolenko, L. A. Kutulyas, V. V. Vashchenko and L. V. Chepeleva, *Liq. Cryst.*, 1994, **16**, 877.
6 A. Ferrarini, G. J. Moro and P. L. Nordio, *Liq. Cryst.*, 1995, **19**, 397.
7 A. Ferrarini, G. J. Moro and P. L. Nordio, *Phys. Rev. E*, 1996, **53**, 681.
8 A. Ferrarini, G. J. Moro and P. L. Nordio, *Mol. Phys.*, 1996, **87**, 485.
9 L. Feltre, A. Ferrarini, F. Pacchiele and P. L. Nordio, *Mol. Cryst. Liq. Cryst.*, 1996, **290**, 109.
10 M. J. Cook and M. R. Wilson, *J. Chem. Phys.*, 2000, **112**, 1560.
11 M. P. Allen, *Phys. Rev. E*, 1993, **47**, 4611.
12 K. M. Aoki and T. Akiyama, *Mol. Cryst. Liq. Cryst.*, 1995, **262**, 543.
13 K. M. Aoki and T. Akiyama, *Mol. Simul.*, 1996, **16**, 99.
14 K. M. Aoki and T. Akiyama, *Mol. Cryst. Liq. Cryst.*, 1997, **299**, 45.
15 D. J. Earl, J. Ilnytskyi and M. R. Wilson, *Mol. Phys.*, 2001, to be published.
16 M. P. Allen and A. Masters, *Mol. Phys.*, 1993, **79**, 277.
17 P. J. Camp, *Mol. Phys.*, 1997, **91**, 381.
18 W. L. Jorgensen and C. Ravimohan, *J. Chem. Phys.*, 1985, **83**, 3050.
19 W. L. Jorgensen, J. M. Briggs and M. L. Contreras, *J. Phys. Chem.*, 1990, **94**, 1683.
20 J. G. Gay and B. J. Berne, *J. Chem. Phys.*, 1981, **74**, 3316.
21 W. L. Jorgensen, D. S. Maxwell and J. Tirado-Rives, *J. Am. Chem. Soc.*, 1996, **118**, 11225.
22 F. J. Vesely, *J. Comput. Phys.*, 1982, **47**, 291.
23 M. R. Wilson, *Liq. Cryst.*, 1996, **21**, 437.
24 M. P. Allen, M. A. Warren, M. R. Wilson, A. Sauron and W. Smith, *J. Chem. Phys.*, 1996, **105**, 2850.

25 G. Gottarelli, G. P. Spada, R. Bartsch, G. Solladie and R. Zimmermann, *J. Org. Chem.*, 1986, **51**, 589.
26 A. Ferrarini, P. L. Nordio, P. V. Shibaev and V. P. Shibaev, *Liq. Cryst.*, 1998, **24**, 219.
27 M. J. Cook and M. R. Wilson, *Liq. Cryst.*, 2000, **27**, 1573.
28 M. J. Cook and M. R. Wilson, *Mol. Cryst. Liq. Cryst.*, 2001, **357**, 149.
29 M. J. Cook and M. R. Wilson, *Mol. Cryst. Liq. Cryst.*, 2001, **357**, 127.
30 D. A. Kofke and P. T. Cummings, *Mol. Phys.*, 1997, **92**, 973.